Accounting for the time evolution of the equation of state parameter during reheating

Pankaj Saha,* Sampurn Anand,† and L. Sriramkumar‡
Department of Physics, Indian Institute of Technology Madras, Chennai 600036, India

(Received 10 May 2020; accepted 21 October 2020; published 11 November 2020)

One of the important parameters in cosmology is the parameter characterizing the equation of state (EOS) of the sources driving the cosmic expansion. Epochs that are dominated by radiation, matter or scalar fields, whether they are probed either directly or indirectly, can be characterised by a unique value of this parameter. However, the EOS parameter during reheating—a phase succeeding inflation which is supposed to rapidly defrost our Universe—remains to be understood satisfactorily. In order to circumvent the complexity of defining an instantaneous EOS parameter during reheating, an effective parameter $w_{\rm eff}$, which is an average of the EOS parameter over the duration of reheating, is usually considered. The value of $w_{\rm eff}$ is often chosen arbitrarily to lie in the range $-1/3 \leq w_{\rm eff} \leq 1$. In this work, we consider the time evolution of the EOS parameter during reheating and relate it to inflationary potentials $V(\phi)$ that behave as ϕ^p around the minimum, a proposal which can be applied to a wide class of inflationary models. We find that, given the index p, the effective EOS parameter $w_{\rm eff}$ is determined uniquely. We discuss the corresponding effects on the reheating temperature and its implications.

DOI: 10.1103/PhysRevD.102.103511

I. INTRODUCTION

In order to explain the current observable Universe, the conventional hot big bang model requires very fine tuned initial conditions during the radiation dominated epoch. This difficulty can be overcome if we assume that the Universe went through a brief phase of nearly exponential expansion—an epoch dubbed as inflation—in its very early stages [1–3]. Apart from explaining the observed extent of isotropy of the cosmic microwave background (CMB) [4–7], inflation also provides a natural mechanism to generate the small anisotropies superimposed on the nearly isotropic background [8–11]. It is these CMB anisotropies which act as the seeds for the eventual formation of the large scale structure in the Universe [12].

But, due to the accelerated expansion, inflation makes the Universe cold and dilute. To be consistent with big bang nucleosynthesis (BBN), the Universe must consist of radiation and matter in thermal equilibrium, when its temperature is around 10 MeV [13–15]. Inflation is typically driven with the aid of scalar fields, often referred to as the inflaton. At the termination of inflation, the energy from the inflaton is supposed to be transferred to the particles constituting the standard model through a process called reheating [16–19]. During this phase of reheating, the inflaton is expected to rapidly decay producing matter and radiation in equilibrium, thereby setting the stage for the conventional hot big bang evolution.

The original mechanism for reheating, suggested soon after the idea of inflation was proposed, was based on the perturbative decay of the inflaton [16–19]. However, about a decade later, it was realized that the perturbative mechanism does not capture the complete picture, as the decay of the inflaton was found to be dominated by nonperturbative processes. Importantly, it was recognized that, immediately after the termination of inflation, the inflaton acts like a coherently oscillating condensate which leads to parametric resonance of the fields coupled to the inflaton [20–24]. In fact, the initial stage of reheating is referred to as preheating, to distinguish it from the later stage of perturbative decay.

The details of the perturbative as well as the nonperturbative processes taking place during reheating can be nontrivial and will actually depend upon the various fields that are taken into account and the nature of their interactions. Moreover, the lack of direct observables that can reveal the dynamics during this phase poses additional challenges towards understanding the mechanism of reheating. In such a situation, as a first step, it would be convenient to characterize the phase through an equation of state (EOS) parameter w which captures the background evolution and, consequently, the dilution of the energy density of the fields involved, without going into the complexity of models and interactions. After all, the different epochs of the Universe—viz. inflation, radiation,

*pankaj@physics.iitm.ac.in
†Present address: Department of Physics, School of Basic and Applied Science, Central University of Tamil Nadu, Thiruvarur 610005, India.
sampurn@cutn.ac.in
‡sriram@physics.iitm.ac.in

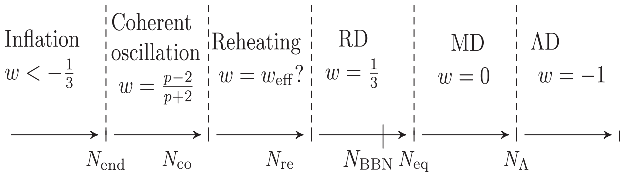

FIG. 1. A schematic timeline of cosmic evolution, with each epoch described by its respective EOS parameter. The quantities $N_{\rm end}$, $N_{\rm BBN}$, $N_{\rm eq}$, and N_{Λ} refer to the e-folds corresponding to the end of inflation, the epochs of BBN, radiation-matter equality and the beginning of Λ domination, respectively. Note that, however, $N_{\rm co}$ and $N_{\rm re}$ refer to the *duration* of the phases of coherent oscillations and reheating.

and matter domination as well as late time acceleration—are often simply characterized in terms of the corresponding EOS parameter (in this context, see Fig. 1). One widely adopted approach is to define an effective EOS parameter $w_{\rm eff}$, which is an average of the instantaneous EOS parameter during the period of reheating [25]. Although the averaging washes out the details of the microphysics over the intermediate stages, it allows us to conveniently characterize the reheating phase in terms of two other vital observables, viz. the duration of the phase and the reheating temperature. While such an approach may be adequate as a first step, needless to add, it is important to characterize and understand the dynamics of reheating in further detail.

As we mentioned, at the end of inflation, the inflaton starts to oscillate about the minimum of the potential. During the initial stages of this phase, most of the energy is stored in the coherently oscillating scalar field. It can be shown that the EOS parameter of a homogeneous condensate oscillating in a potential which has a minimum of the form $V(\phi) \propto \phi^p$ is given by $w_{\rm co} = (p-2)/(p+2)$ [26–28]. (For a brief discussion in this context for the case of $p = 2$, see the Appendix.) However, in the process, the homogeneous condensate fragments leading to the growth of the inhomogeneities [29–32]. As a result, the EOS parameter differs from the above-mentioned form. The time when the EOS starts to change from its form during the period of coherent oscillations is referred to in the literature as the onset of the phase of backreaction [33,34]. The effects of fragmentation on the EOS can be studied using lattice simulations, and one finds that the EOS parameter indeed eventually approaches that of the radiation dominated phase (i.e., $w \to 1/3$) as required [34–36]. Evidently, the average $w_{\rm eff}$ during reheating will depend on the time evolution of the EOS parameter from the end of coherent oscillations to the start of the radiation domination epoch. Usually, the value of $w_{\rm eff}$ during this phase is either identified to be the value $w_{\rm co}$ during the coherent oscillation phase or chosen arbitrarily to lie in the range $-1/3 \leq w_{\rm eff} \leq 1$ [37].

In this work, we examine the time evolution of the EOS parameter and its average $w_{\rm eff}$ during reheating. We consider the time evolution of the EOS from the end of the coherent oscillation stage until the onset of the radiation domination epoch. We argue that the presence of gradient and/or interaction energy of the inflaton leads to the deviation of the EOS parameter from its value $w_{\rm co}$ during the period of coherent oscillations. Not surprisingly, we find that, even after the phase of coherent oscillations, the shape the inflationary potential near its minimum plays a role in the time evolution of the EOS. We shall assume that, near their minima, the inflationary models of our interest have the following form: $V(\phi) \propto \phi^p$. We should point out here that large field models which are *completely* described by such power law potentials are already ruled out due to the constraints from the CMB data on the primary inflationary observables, viz. the scalar spectral index $n_{\rm S}$ and tensor-to-scalar ratio r [38–40]. In contrast, potentials that contain a plateau, such as the original Starobinsky model, which lead to smaller values of r are favored by the CMB data. However, such potentials too can be expressed as $V(\phi) \propto \phi^p$ around the minima (in this context, see Fig. 2 wherein we have schematically illustrated the potentials for $p = 2$). Motivated by results from lattice simulations, in order to capture the microphysics during reheating and, specifically, the turbulent backreaction phase, we propose an evolving EOS parameter, which asymptotically approaches its value during the radiation dominated epoch from its value at the end of the phase of coherent oscillations. With such a time evolving EOS parameter, we establish a link between the value of $w_{\rm eff}$ and the inflationary potential parameters. This allows us to connect the reheating temperature uniquely

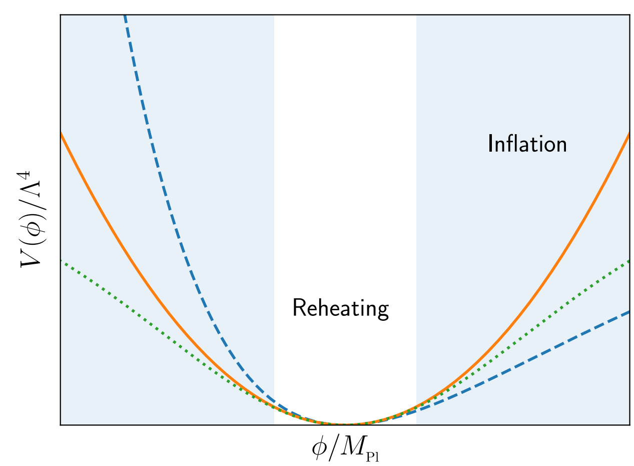

FIG. 2. A schematic diagram illustrating the behavior of typical inflationary potentials of our interest around their minima. We have plotted the potentials for the cases of the Starobinsky model (in blue), the so-called α-attractor T model (in green) and the quadratic potential (in orange). Away from the minimum, at large field values, the presence of a plateau in the potentials (such as in the Starobinsky and T models) ensure that the inflationary predictions are consistent with the CMB observations. Around the minimum, the potentials behave as $V(\phi) \propto \phi^p$, which permits coherent oscillations during the initial stages of reheating.

to the inflationary parameters, while, importantly, accounting for the time evolution of the EOS.

The remainder of the paper is structured as follows. In Sec. II, we shall provide a rapid overview of reheating and connect the parameters describing the phase with the observables in the CMB. In Sec. III, we shall first briefly highlight the motivations for accounting for the time-dependence of the EOS during reheating. With the help of specific examples, we shall also present results from lattice simulations illustrating the time evolution of the EOS parameter from the end of the coherent oscillation phase to the onset of the radiation dominated epoch. We shall then go on to consider two types of parametrizations for the EOS parameter and arrive at the associated effective EOS parameter. In Sec. IV, we shall apply these arguments to the so-called α-attractor model of inflation and evaluate the corresponding reheating temperatures for these models. We shall conclude with a brief summary of our results in Sec. V.

II. CONNECTING THE REHEATING PHASE WITH THE CMB OBSERVABLES

While the period of reheating is phenomenologically rich, as we mentioned, it is difficult to observationally constrain the dynamics due to the paucity of direct access to that epoch. Another difficulty arises due to the fact that by the time of BBN, all the particles associated with the standard model are expected to have been thermalized, thereby possibly hiding away the details of their production. Despite these limitations, one finds that reheating can still be constrained to a certain extent from the CMB and BBN observables. The upper bound on the inflationary energy scale, inferred from the constraints on the tensor-to-scalar ratio r (arrived at originally from the WMAP data [38] and improved upon later by the Planck data [39,40]), is closer to the scale of grand unified theory (GUT) which is of about 10^{16} GeV, whereas BBN requires a radiation dominated universe at around 10 MeV [13–15]. The inflationary observables are either well measured or have bounds on them, while the physics of BBN have been tested with great precision. Thus, there is a huge window in energy scales of several order of magnitudes which remains unconstrained by the cosmological data.

However, as has been pointed out in the literature, a connection can be made between the reheating phase and the CMB observables measured today [37,41,42]. As it proves to be essential for our discussion later on, we shall quickly summarize the primary arguments in this section. Recall that, during inflation, a scale of interest described by the comoving wave number k leaves the Hubble radius at the time when $k = a_k H_k$. Let this time correspond to, say, N_k, e-folds before the end of inflation. For instance, the Planck team choose their pivot scale to be $k = 0.05\ \mathrm{Mpc}^{-1}$ and *assume* $N_k \simeq 50$ for this scale [39,40]. The physical wave number k/a_k at the time when it exits the Hubble radius during inflation can be related to its corresponding value k/a_0 at the present time as follows:

$$\frac{k}{a_k H_k} = \frac{k}{a_0 H_k}\frac{a_0}{a_{\mathrm{re}}}\frac{a_{\mathrm{re}}}{a_{\mathrm{co}}}\frac{a_{\mathrm{co}}}{a_{\mathrm{end}}}\frac{a_{\mathrm{end}}}{a_k}, \tag{1}$$

where a_{end}, a_{co}, and a_{re} are the values of the scale factor when inflation, the phase of coherent oscillations and reheating end, respectively. Since $\mathrm{e}^{N_k} = a_{\mathrm{end}}/a_k$, $\mathrm{e}^{N_{\mathrm{co}}} = a_{\mathrm{co}}/a_{\mathrm{end}}$, and $\mathrm{e}^{N_{\mathrm{re}}} = a_{\mathrm{re}}/a_{\mathrm{co}}$, we can express the above equation as

$$N_k + N_{\mathrm{co}} + N_{\mathrm{re}} + \ln\left(\frac{a_0}{a_{\mathrm{re}}}\right) + \ln\left(\frac{k}{a_0 H_k}\right) = 0, \tag{2}$$

where, evidently, N_{co} and N_{re} denote the *durations* of the phase of coherent oscillations and the backreaction phase.

At the end of reheating, the Universe is supposed to be radiation dominated and if no significant entropy is released into the primordial plasma, we can relate the reheating temperature, say, T_{re}, to the present CMB temperature, say, T_0, as follows (see, for example, Ref. [37]):

$$\frac{T_{\mathrm{re}}}{T_0} = \left(\frac{43}{11 g_{\mathrm{s,re}}}\right)^{1/3}\frac{a_0}{a_{\mathrm{re}}}, \tag{3}$$

where $g_{\mathrm{s,re}}$ denotes the effective number of relativistic degrees of freedom that contribute to the entropy during reheating. We should mention that, to arrive at the above expression, we have expressed the neutrino temperature in terms of the temperature T_0 of the CMB using the relation $T_{\nu 0} = (4/11)^{1/3} T_0$. On using Eqs. (2) and (3), we can express the reheating temperature as

$$T_{\mathrm{re}} = \left(\frac{43}{11 g_{\mathrm{s,re}}}\right)^{1/3}\left(\frac{a_0 T_0}{k}\right) H_k \mathrm{e}^{-N_k}\mathrm{e}^{-N_{\mathrm{co}}}\mathrm{e}^{-N_{\mathrm{re}}}. \tag{4}$$

Let us now assume that the backreaction phase succeeding the period of coherent oscillations is described by the time-dependent EOS parameter $w(N)$. In such a case, from the conservation of energy, the cosmic energy density during the phase can be expressed as

$$\rho(N) = \rho_{\mathrm{co}} \exp\left\{-3\int_0^N \mathrm{d}N'[1 + w(N')]\right\}, \tag{5}$$

where ρ_{co} is the energy density at the end of the coherent oscillation phase. On defining an averaged EOS parameter as

$$w_{\mathrm{eff}} = \frac{1}{N_{\mathrm{re}}}\int_0^{N_{\mathrm{re}}} \mathrm{d}N' w(N'), \tag{6}$$

we can rewrite the above expression as

$$\ln\left(\frac{\rho_{co}}{\rho_{re}}\right) = 3(1+w_{eff})N_{re}, \qquad (7)$$

where N_{re} denotes the number of e-folds *during* the backreaction phase counted from the end of the period of coherent oscillations.

If we now assume that, at the end of reheating, the dominant component of energy is radiation, then we can express the energy density of radiation in terms of T_{re} as

$$\rho_{re} \equiv \rho_\gamma(T_{re}) = \frac{\pi^2 g_{re}}{30} T_{re}^4, \qquad (8)$$

where g_{re} is the number of effective relativistic degrees of freedom at the end of reheating. In such a case, upon using Eqs. (7) and (8), we can readily express T_{re} as

$$T_{re} = \left(\frac{30\rho_{co}}{g_{re}\pi^2}\right)^{1/4} \exp\left[-\frac{3}{4}(1+w_{eff})N_{re}\right]. \qquad (9)$$

From Eqs. (4) and (9), we can then arrive at the following expression for the duration N_{re} of the phase of reheating:

$$N_{re} = \frac{4}{3w_{eff}-1}\left[N_k + N_{co} + \ln\left(\frac{k}{a_0 T_0}\right) + \frac{1}{4}\ln\left(\frac{30}{\pi^2 g_{re}}\right) + \frac{1}{3}\ln\left(\frac{11 g_{s,re}}{43}\right) - \ln\left(\frac{H_k}{\rho_{end}^{1/4}}\right) - \frac{1}{4}\ln\left(\frac{\rho_{end}}{\rho_{co}}\right)\right], \qquad (10)$$

where ρ_{end} is the energy density of the inflaton at the end of inflation. Since the EOS parameter during the phase of coherent oscillations is $w_{co} = (p-2)/(p+2)$, which is obviously a constant for given value of p, we can express ρ_{co} in terms of ρ_{end} as

$$\ln\left(\frac{\rho_{end}}{\rho_{co}}\right) = 3\left(1+\frac{p-2}{p+2}\right)N_{co}. \qquad (11)$$

Therefore, the duration of reheating N_{re} can finally be expressed as

$$N_{re} = \frac{4}{3w_{eff}-1}\left[N_k + \frac{(4-p)}{2(p+2)}N_{co} + \ln\left(\frac{k}{a_0 T_0}\right) + \frac{1}{4}\ln\left(\frac{30}{\pi^2 g_{re}}\right) + \frac{1}{3}\ln\left(\frac{11 g_{s,re}}{43}\right) - \ln\left(\frac{H_k}{\rho_{end}^{1/4}}\right)\right]. \qquad (12)$$

During inflation, the energy density of the inflaton can be expressed in terms the potential $V(\phi)$ and the first slow roll parameter $\epsilon = -\dot{H}/H^2$ as

$$\rho = V\left(1+\frac{\epsilon}{3-\epsilon}\right). \qquad (13)$$

Since inflation ends when $\epsilon = 1$, we have $\rho_{end} = (3/2)V_{end}$, where V_{end} denotes the potential at ϕ_{end}, viz. the value of the scalar field at which inflation is terminated. Given the potential $V(\phi)$, the value of ϕ_{end} can be readily determined using the condition $\epsilon \simeq (M_{Pl}^2/2)(V_\phi/V)^2 = 1$, where the subscript on the potential denotes the derivative with respect to the scalar field. Also, working in the slow roll approximation, we can calculate the value of the scalar field at N_k. This, in turn, can be utilized to express N_k in terms of the inflationary observables, viz. the scalar spectral index n_S and tensor-to-scalar ratio r. Therefore, the bounds on the inflationary parameters from the CMB will lead to the corresponding constraints on the reheating parameters as well (in this context, see Refs. [37,42–50]). However, note that the quantity N_{co} depends on the details of the inflationary model under investigation and, importantly, on the coupling of the inflaton to the other fields.

III. TIME-DEPENDENT EOS

As discussed earlier, the EOS parameter for the homogeneous condensate, oscillating about the minimum of a potential behaving as $V(\phi) \propto \phi^p$, is given by $w_{co} = (p-2)/(p+2)$ [26,27]. However, due to the growth of inhomogeneities, the EOS parameter can be expected to differ from the above value during the backreaction phase. We can study the resulting variation in the EOS parameter by considering virialization of the inhomogeneous system in equilibrium.

Consider a situation wherein the inflaton ϕ decays into daughter fields collectively represented as $\mathcal{F}$ through the interaction potential $V_I(\phi, \mathcal{F})$. For a potential that behaves as $V(\phi) \propto \phi^p$ near its minimum, one can show that, in equilibrium, the following virial relations between the kinetic, potential and the interaction energy densities hold (in this context, see, for example, Refs. [34–36]):

$$\frac{1}{2}\langle\dot{\phi}^2\rangle = \frac{1}{2}\left\langle\frac{|\nabla\phi|^2}{a^2}\right\rangle + \frac{p}{2}\langle V(\phi)\rangle + \langle V_I(\phi,\mathcal{F})\rangle, \qquad (14a)$$

$$\frac{1}{2}\langle\dot{\mathcal{F}}^2\rangle = \frac{1}{2}\left\langle\frac{|\nabla\mathcal{F}|^2}{a^2}\right\rangle + \langle V_I(\phi,\mathcal{F})\rangle, \qquad (14b)$$

where the angular brackets indicate that the quantities have been averaged over space as well as the period of oscillation of the inflaton. During this backreaction phase, one can define the instantaneous EOS averaged over the spatial volume as

$$w = \frac{\frac{1}{2}\dot{\phi}^2 + \frac{1}{2}\dot{\mathcal{F}}^2 - \frac{1}{6a^2}|\nabla\phi|^2 - \frac{1}{6a^2}|\nabla\mathcal{F}|^2 - V_I(\phi,\mathcal{F})}{\frac{1}{2}\dot{\phi}^2 + \frac{1}{2}\dot{\mathcal{F}}^2 + \frac{1}{2a^2}|\nabla\phi|^2 + \frac{1}{2a^2}|\nabla\mathcal{F}|^2 + V_I(\phi,\mathcal{F})}. \qquad (15)$$

Upon using the virial relations (14), we find that the above expression for w reduces to

$$w = \frac{1}{3} + \left(\frac{p-4}{6}\right)\left(\frac{p+2}{4} + \frac{\langle\rho_{\mathrm{G}}\rangle}{\langle V(\phi)\rangle} + \frac{3\langle V_{\mathrm{I}}(\phi,\mathcal{F})\rangle}{2\langle V(\phi)\rangle}\right)^{-1}, \tag{16}$$

where $\langle\rho_{\mathrm{G}}\rangle = \langle|\nabla\phi|^2/(2a^2)\rangle + \langle|\nabla\mathcal{F}|^2/(2a^2)\rangle$ is the total energy density associated with the spatial gradients in the fields.

It should be clear from the above equation for w that, as the gradient and the interaction energies begin to dominate, the second term in the expression becomes insignificant and the EOS parameter approaches $1/3$. To explicitly demonstrate these effects of the gradient and interaction energy densities on the EOS parameter, in Fig. 3, we have plotted the contours of fixed w from Eq. (16) for potentials $V(\phi)$ which behave as ϕ^2 and ϕ^6 around their minima. There are two points that should be evident from the figure. First, even a slight increase in the gradient or interaction energy densities results in a nonzero instantaneous EOS parameter. Second, as we pointed out above, w asymptotically approaches $1/3$, as both the gradient and interaction energy densities increase. As we shall illustrate in the following subsection, these expectations are corroborated by lattice simulations which allows one to track the EOS from the end of the phase of coherent oscillations to the beginning of the radiation dominated epoch (in this context, also see, for instance, Refs. [34–36]). These simulations suggest that, for $p < 4$, the EOS parameter monotonically increases towards the asymptotic value of $1/3$. Similarly, for $p > 4$, one finds that it decreases monotonically towards $1/3$. From these arguments, we conclude that, in any realistic scenario, the EOS during reheating must be different than its value during the phase of coherent oscillations and that a vanishing EOS parameter is highly unlikely during this stage.

A. Specific examples of the time-dependent EOS

In order to understand the typical form of the evolution of the EOS parameter, in this subsection, we shall present the results of lattice simulations for a specific model. We shall work with the so-called α-attractor T models whose potentials are given by [51]

$$V(\phi) = \Lambda^4 \left|\tanh^p\left(\frac{\phi}{\sqrt{6\alpha}M_{\mathrm{Pl}}}\right)\right|. \tag{17}$$

We shall assume that the inflaton decays into a lighter scalar degree of freedom via a coupling of the form $(g^2/2)\phi^2\chi^2$. For the values of the parameter α such that $\alpha \gtrsim 1$, the preheating dynamics in the above models are identical to that of the power law chaotic potentials $V(\phi) \propto |\phi|^p$ (in this context, also see Refs. [35,36,49]). With the above forms of the potential and interaction, we have solved for the coupled scalar field dynamics on a 256^3 lattice using the parallel version of the lattice simulation code LATTICEEASY [52,53]. We have set $\alpha = 1$ and

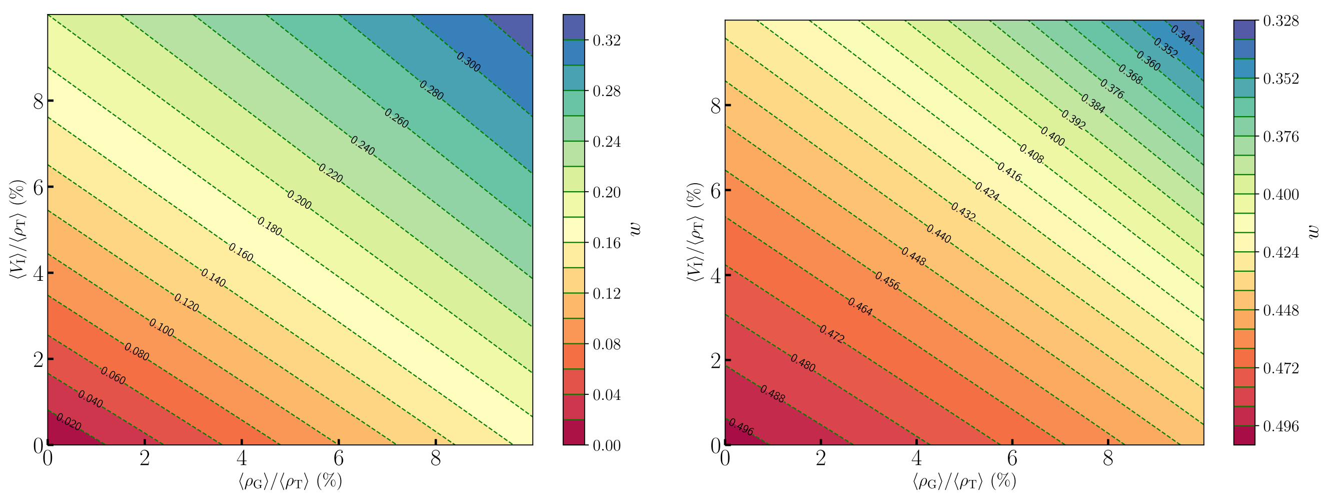

FIG. 3. The contours corresponding to constant EOS parameter w during reheating—as defined by Eq. (16)—have been plotted in the $\langle\rho_{\mathrm{G}}\rangle$-$\langle V_{\mathrm{I}}\rangle$ plane for the case of potentials $V(\phi)$ which behave as ϕ^2 (on the left) and ϕ^6 (on the right) near their minima. In order to make the axes dimensionless, we have divided both the axes by the quantity $\langle\rho_{\mathrm{T}}\rangle$, which represents the total energy density of the inflaton as well as the daughter fields. In plotting these contours, based on the results from lattice simulations, we have assumed that the kinetic energy density constitutes 70% of the total energy density $\langle\rho_{\mathrm{T}}\rangle$ [34]. However, we should hasten to add that changing the level of contribution due to the kinetic energy density does not alter the qualitative nature of the plots. As we have discussed, the transfer of energy to the daughter fields as well as the growth of inhomogeneities occur rapidly at the end of the phase of coherent oscillations [35,36]. Note that the plots clearly indicate that, as the contributions due to the gradient and the interaction energy densities increase, w moves away from zero and eventually approaches $1/3$.

$g^2 = 3.5 \times 10^{-7}$, and have considered the following five different values for the index describing the above potential: $p = (2, 3, 4, 5, 6)$. In these runs, the initial conditions for the background are set at the instant when the inflaton begins to oscillate near the bottom of the potential. The EOS parameter for the above two-field system is obtained using Eq. (15). In Fig. 4, we have plotted the variation of the oscillation averaged EOS parameter against the number of e-folds from the time when we start the simulations. As expected, we observe that, during the initial coherent oscillation phase, the EOS parameter is given by $w_{\rm co} = (p-2)/(p+2)$. The EOS parameter begins to change once the inhomogeneities start to grow and it gradually tends towards $w = 1/3$ in all the cases except for $p = 2$. We should point out that similar results from lattice simulations have also been arrived at earlier (see, for instance, Ref. [54]). For the case of $p = 2$, in the scenario involving two fields, one finds that the final stage ends up being dominated by the inflaton itself, which restricts the EOS parameter from approaching radiationlike behavior. Similar behavior has also been encountered when one takes into account only the self-resonance of the inflaton [35,36]. However, the result for the case of $p = 2$ must be viewed as a limitation of the specific coupling and, as the results for the other cases of p suggest, reheating can be expected to bring about a radiation dominated universe. We must note that, in any realistic situation, reheating must lead to a radiation dominated phase, else one has to invoke an additional mechanism such as perturbative reheating to come to our aid. The main goal of these lattice simulations is to motivate the construction of time-dependent EOS parameter to describe the epoch of reheating. In the following subsection, we shall discuss time-dependent EOS parameters which effectively capture the results we have obtained from the end of the coherent oscillation phase until the beginning of the epoch of radiation domination.

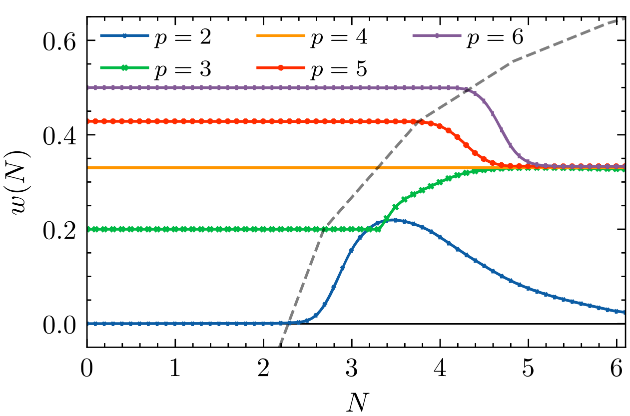

FIG. 4. The EOS parameter obtained from lattice simulations for the alpha-attractor T models described by the potential (17) has been plotted as a function of e-folds for the cases wherein $p = (2, 3, 4, 5, 6)$. Notice that the EOS parameter starts with the value of $w_{\rm co} = (p-2)/(p+2)$ and approaches $w = 1/3$ in all the cases apart from the case of $p = 2$. In the case of $p = 2$, it is known that the specific coupling we have considered is not effective to achieve radiation domination [49]. Utilizing Eq. (33), in the figure, we have also plotted $w_{\rm co} = (p-2)/(p+2)$ against $N_{\rm co}$ (as a dashed black curve) for the case of $R_{\rm co} = 25$. The locations of the intersection of the curve with the EOS parameter indicate the onset of the backreaction phase for the different indices p.

B. Parametrizing the EOS

Motivated by the results from the lattice simulations, in order to capture the continuous variation of the EOS parameter from the end of coherent oscillations to radiation domination, we shall now parametrize the instantaneous EOS parameter *by hand* n terms of e-folds. In choosing the functional form of the EOS parameter, we assume that it varies monotonically from its initial value $w_{\rm co}$ to the final value of $1/3$. We find that this condition considerably restricts the form of the functions we can consider.

We consider two different parametrizations of the following forms:

(1) Case A: exponential form

$$w(N) = w_0 + w_1 \exp\left(-\frac{1}{\Delta}\frac{N}{N_{\rm re}}\right), \qquad (18)$$

(2) Case B: tan-hyperbolic form

$$w(N) = w_0 + w_1 \tanh\left(\frac{1}{\Delta}\frac{N}{N_{\rm re}}\right), \qquad (19)$$

where N is the number of e-folds counted from the end of the phase of coherent oscillations. We must clarify here that although, we have used the same symbols w_0, w_1, and Δ in the two parametrizations, *a priori*, we do not expect that two sets of parameters are related or that the functional dependence of $w(N)$ on them are similar. The parameters w_0 and w_1 are fixed from the values of w at the end of the coherent oscillations and the asymptotic limit which we take to be that of the radiation dominated epoch. Evidently, the parameter Δ controls the efficiency of the reheating process and determines how quickly the radiation dominated phase is attained. We further assume that the EOS parameter at the end of reheating, say, $w_{\rm re}$, is within 10% of the asymptotic value of $1/3$. There are two reasons for this assumption. The first is the reason that one has to account for various physical effects that can result in the deviation of the EOS parameter from $1/3$ during the initial stages of radiation domination (see Ref. [55]; in this context, also see Ref. [56], Sec. 2.11). The second is the practical reason to set a benchmark where the energy density of radiation has formally begun to dominate the rest of the energy densities. We find that this choice of $w_{\rm re}$ fixes the value of Δ. Under these conditions, the two parametrizations take the following form:

$$w(N,p) = \begin{cases} \frac{1}{3} + \frac{2}{3}\left(\frac{p-4}{p+2}\right)\exp\left(-\frac{1}{\Delta}\frac{N}{N_{\rm re}}\right), & \text{(A)} \\ \frac{p-2}{p+2} - \frac{2}{3}\left(\frac{p-4}{p+2}\right)\tanh\left(\frac{1}{\Delta}\frac{N}{N_{\rm re}}\right), & \text{(B)} \end{cases} \tag{20}$$

with

$$\frac{1}{\Delta} = \begin{cases} \ln\left[\left(\frac{p-4}{p+2}\right)\left(\frac{2}{3w_{\rm re}-1}\right)\right], & \text{(A)} \\ \tanh^{-1}\left\{\frac{3}{2}\left[\frac{p-2-w_{\rm re}(p+2)}{p-4}\right]\right\}. & \text{(B)} \end{cases} \tag{21}$$

We had already pointed out that, from its initial value of $w_{\rm co} = (p-2)/(p+2)$, the EOS parameter w increases or decreases monotonically towards $1/3$ for $p < 4$ and $p > 4$, respectively. For $p = 4$, the reheating phase is indistinguishable from the radiation dominated epoch since $w_{\rm co} = 1/3$. Hence, in such a case, $\Delta \to 0$. In Fig. 5, we have compared the two parametrizations described by Eq. (20) for different values of p. Note that the behavior of two parametrizations are qualitatively similar and, importantly, they broadly mimic the behavior we had seen in the results from lattice simulations we had discussed in the previous subsection.

Given the forms (20) for the time varying EOS parameter, we can determine the corresponding $w_{\rm eff}$ [cf. Eq. (6)] for the two cases A and B to be

$$w_{\rm eff}(p) = \begin{cases} \frac{1}{3} - \frac{2\Delta}{3}\left(\frac{p-4}{p+2}\right)(e^{-1/\Delta} - 1), & \text{(A)} \\ \left(\frac{p-2}{p+2}\right) - \frac{2\Delta}{3}\left(\frac{p-4}{p+2}\right)\log\left[\cosh\left(1/\Delta\right)\right]. & \text{(B)} \end{cases} \tag{22}$$

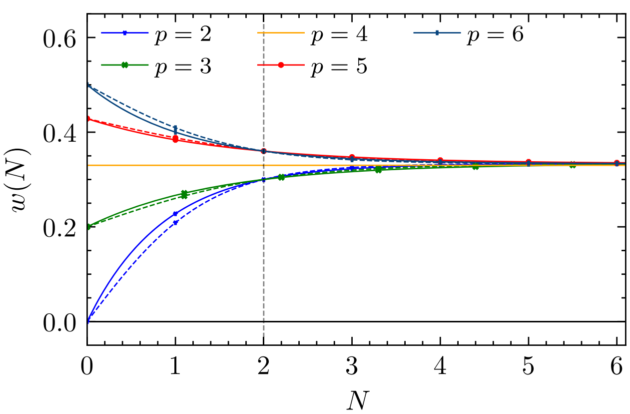

FIG. 5. The time-dependent EOS parameter $w(N)$ during reheating has been plotted as a function of e-folds when the inflaton evolves in potentials which behave as $V(\phi) \propto \phi^p$ near their minima. We have plotted both the exponential (as solid lines) and the tan-hyperbolic (as dashed lines) parametrizations that we have proposed [cf. Eq. (20)] for a few different values of p. As a benchmark, we take the end of reheating (denoted by the red vertical line) to be when the EOS parameter reaches within 10% of its asymptotic value of $1/3$.

TABLE I. Comparison between the EOS parameter during coherent oscillations $w_{\rm co}$ and the effective EOS parameter $w_{\rm eff}$ during reheating for the two parametrizations that we have proposed. Clearly, $w_{\rm eff}$ is largely independent of the two parametrizations we have considered. Also, note that, in general, $w_{\rm eff}$ proves to be substantially different from $w_{\rm co}$.

p	$w_{\rm co}$	$w_{\rm eff}^{\rm exp}$	$w_{\rm eff}^{\rm tanh}$
1	$-1/3$	0.12	0.09
2	0	0.20	0.19
4	$1/3$	$1/3$	$1/3$
6	$1/2$	0.41	0.42
8	$3/5$	0.44	0.45
$p \to \infty$	1	0.53	0.56

Thus, for a given inflationary potential, $w_{\rm eff}$ is fixed. In Table I, we have compared the values of $w_{\rm eff}$ for the two parametrizations with the value of $w_{\rm co}$ for a set of values of p. On substituting Eq. (22) for $w_{\rm eff}$ in Eq. (10) for $N_{\rm re}$, we obtain that

$$N_{\rm re} = \begin{cases} 2\left(\frac{p+2}{p-4}\right)\mathcal{N}[\Delta(1-e^{-1/\Delta})]^{-1}, & \text{(A)} \\ 2\left(\frac{p+2}{p-4}\right)\mathcal{N}\{1-\Delta\log\left[\cosh(1/\Delta)\right]\}^{-1}, & \text{(B)} \end{cases} \tag{23}$$

where the quantity $\mathcal{N}$ is defined as

$$\mathcal{N} = N_k + \frac{(4-p)}{2(p+2)}N_{\rm co} + \ln\left(\frac{k}{a_0 T_0}\right) + \frac{1}{4}\ln\left(\frac{30}{\pi^2 g_{\rm re}}\right) + \frac{1}{3}\ln\left(\frac{11 g_{\rm s,re}}{43}\right) - \ln\left(\frac{H_k}{\rho_{\rm end}^{1/4}}\right), \tag{24}$$

while Δ is given by Eq. (21). It should be clear from the above equation that, barring $g_{\rm re}$, $g_{\rm s,re}$, and $N_{\rm co}$, the duration of reheating $N_{\rm re}$ depends only on the inflationary parameters and the CMB observables. On substituting the above expressions for $w_{\rm eff}$ and $N_{\rm re}$ in Eq. (9), we can arrive at the corresponding reheating temperature $T_{\rm re}$.

IV. APPLICATION TO AN INFLATIONARY MODEL

Let us now apply our arguments to an inflationary model which has the desired behavior near its minima. Towards this end, we shall consider the so-called α-attractor model described by potential [57,58]

$$V(\phi) = \Lambda^4\left[1 - \exp\left(-\sqrt{\frac{2}{3\alpha}}\frac{\phi}{M_{\rm Pl}}\right)\right]^p, \tag{25}$$

where Λ, α, and p are, evidently, parameters that characterize the model. As we had pointed out, we can express the first slow roll parameter as $\epsilon \simeq (M_{\rm Pl}^2/2)(V_\phi/V)^2$, where the subscript ϕ denotes the derivative of the potential with respect to the field. Let us define the second slow roll parameter as $\eta \simeq M_{\rm Pl}^2(V_{\phi\phi}/V)$. Then, in the slow roll approximation, the inflationary observables—viz. the scalar spectral index $n_{\rm S}$ and the tensor-to-scalar ratio r—can be expressed in terms of these parameters as (see, for instance, the reviews [59–67])

$$n_{\rm S} = 1 - 6\epsilon_k + 2\eta_k, \tag{26a}$$

$$r = 16\epsilon_k, \tag{26b}$$

where the subscript k indicates that these quantities have to be evaluated when the mode leaves the Hubble radius. Moreover, the scalar amplitude $A_{\rm S}$ can be expressed in terms of the value of the Hubble parameter H_k and the tensor-to-scalar ratio r as follows:

$$H_k = \sqrt{\frac{rA_s}{2}}\pi M_{\rm Pl}. \tag{27}$$

The number of e-folds N_k between the mode k leaving the Hubble radius and the end of inflation can be expressed in the slow roll approximation as

$$N_k = \int_{\phi_k}^{\phi_{\rm end}} {\rm d}\phi \frac{H}{\dot\phi} \simeq \frac{1}{M_{\rm Pl}^2}\int_{\phi_{\rm end}}^{\phi_k} {\rm d}\phi \frac{V}{V_\phi}. \tag{28}$$

For the inflationary potential (25) of our interest, N_k can be evaluated to be

$$N_k = \frac{3\alpha}{2p}\left[\exp\left(\sqrt{\frac{2}{3\alpha}}\frac{\phi_k}{M_{\rm Pl}}\right) - \exp\left(\sqrt{\frac{2}{3\alpha}}\frac{\phi_{\rm end}}{M_{\rm Pl}}\right) - \sqrt{\frac{2}{3\alpha}}\frac{(\phi_k - \phi_{\rm end})}{M_{\rm Pl}}\right]. \tag{29}$$

The quantity $\phi_{\rm end}$ can be determined by the condition $\epsilon = 1$ and is given by

$$\frac{\phi_{\rm end}}{M_{\rm Pl}} = \sqrt{\frac{3\alpha}{2}}\ln\left(1 + \frac{p}{\sqrt{3\alpha}}\right), \tag{30}$$

so that we have

$$V_{\rm end} = V(\phi_{\rm end}) = \Lambda^4\left(\frac{p}{p + \sqrt{3\alpha}}\right). \tag{31}$$

The above relations between ϕ_k, $\phi_{\rm end}$, and N_k and Eq. (26a) for the scalar spectral index allows us to write $n_{\rm S}$ in terms of N_k. We can then invert the relation to express N_k in terms of $n_{\rm S}$.

Note that, near its minimum, the inflationary potential (25) can be approximated as

$$V(\phi) \simeq \Lambda^4\left(\frac{2\phi}{3\alpha M_{\rm Pl}}\right)^p, \tag{32}$$

which is of the form we desire. We should mention here that, for $\alpha = 1$ and $p = 2$, the potential (25) corresponds to the Starobinsky model, which is the most favored model according to the recent CMB observations [39,40]. Recall that, for a given p, $w_{\rm eff}$ is fixed [cf. Eq. (22)]. Hence, we have most of the required ingredients to calculate the duration of reheating $N_{\rm re}$ and the corresponding reheating temperature $T_{\rm re}$ using the expressions (23) and (9). However, we shall require values for $g_{\rm re}$, $g_{\rm s,re}$, and $N_{\rm co}$. It seems reasonable to choose $g_{\rm re} = g_{\rm s,re} = 10^2$ [27].

Let us now turn to identifying a suitable choice for $N_{\rm co}$. The duration of the phase of coherent oscillation can strongly depend on the model parameters and, importantly, on the couplings of the inflaton to other fields [33]. In particular, if nonperturbative processes dominate throughout the reheating phase, thermalization may be achieved within a few e-folds making it difficult to connect the reheating phase with the CMB observables. However, this phase can be inefficient or delayed [68–70] and can result in the breakdown of coherent oscillations without thermalization [71,72]. It has been pointed out that the final stage of reheating must involve the perturbative decay of the inflaton and the thermalization is slow if we, for example, invoke certain supersymmetric extensions of the standard model to achieve inflation [73]. Although preheating can generate a plasma of inflaton and other daughter fields in kinetic equilibrium, complete thermal equilibrium is achieved over a much larger time scale than that of the preheating [30,74]. The exact number for $N_{\rm co}$ will depend on the inflationary potential as well as the type of interaction(s) and the strength of the coupling parameter (s). However, if there are no daughter fields present and inflaton fragments only due to self-resonance, one can arrive at an estimate for the upper bound on its value, which is found to be (see Refs. [35,36])

$$N_{\rm co} \simeq \frac{(p+2)}{6}\ln R_{\rm co}, \tag{33}$$

where $R_{\rm co} \sim \mathcal{O}(10^2)$ depends on the resonance structure. On assuming $R_{\rm co}$ to be 10^2, we get $N_{\rm co} = (3.07, 4.60, 6.14)$ for $p = (2, 4, 6)$. If coupling to other fields are present, the value of $N_{\rm co}$ will naturally decrease [33]. Therefore, the period of preheating is negligible compared to the entire duration of reheating. Due to these reasons, we consider $N_{\rm co}$ to be small and set it to unity.

With all these necessary ingredients at hand, let us now compute the reheating temperature $T_{\rm re}$ for the model of our interest. Note that, $T_{\rm re}$ depends on $n_{\rm S}$, p, α, and $w_{\rm eff}$. We shall set $\alpha = 1$ without any loss of generality. Since $w_{\rm eff}$ is largely independent of the two parametrizations (cf. Table I), we shall choose to work with the values corresponding to the exponential form for $w(N)$. In Fig. 6, we have highlighted the dependence of $T_{\rm re}$ on $n_{\rm S}$ and p in two different manner. We have first plotted $T_{\rm re}$ as a function of p for the value of $n_{\rm S}$ that leads to the best fit to the recent

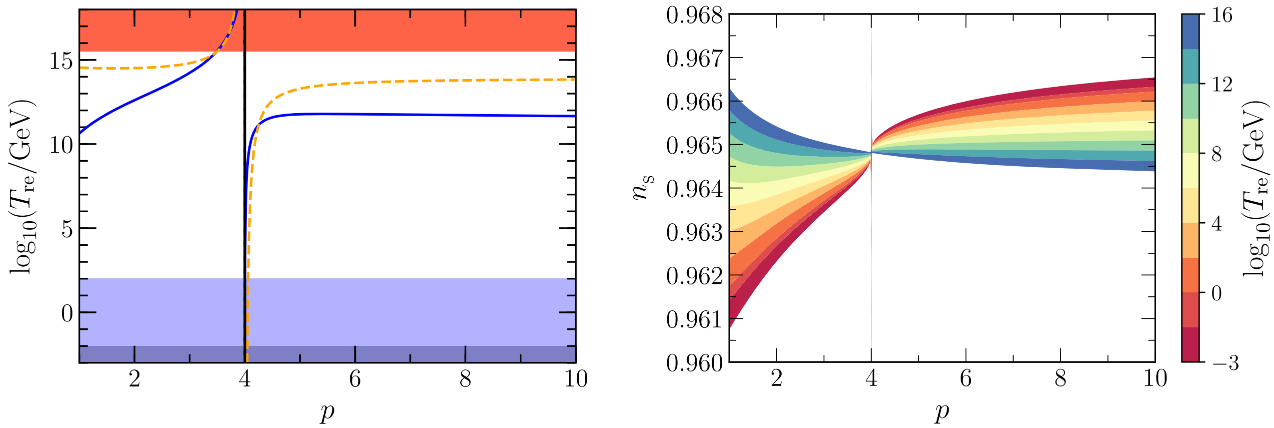

FIG. 6. The dependence of the reheating temperature $T_{\rm re}$ on the index p has been illustrated (on the left) for $n_{\rm S} = 0.9649$ which leads to the best-fit to the CMB data [39,40]. We have plotted the dependence of $T_{\rm re}$ on p for $w_{\rm eff}$ corresponding to the exponential parametrization [cf. Eqs. (20) and (22)] (as the solid blue curve) as well as for the choice $w_{\rm eff} = w_{\rm co} = (p-2)/(p+2)$ (as the dashed orange curve). We have also indicated the following domains (in the figure on the left): the region above maximum possible reheating temperature of $T_{\rm inst} = [30\rho_{\rm end}/(g_{\rm re}\pi^2)]^{1/4}$ corresponding instantaneous reheating or $N_{\rm re} = 0$ (in red), the domains below the electroweak scale taken to be $T_{\rm EW} \sim 100$ GeV (in lighter blue) and the region below 10 MeV, which is the minimum temperature required for BBN (in darker blue). Moreover, we have illustrated the dependence of $T_{\rm re}$ on $n_{\rm S}$ and p (on the right) for the choice of $w_{\rm eff}$ corresponding to the exponential parametrization. Note that we have set $\alpha = 1$ in both these plots.

CMB data [39,40]. In the figure, we have also illustrated the simultaneous dependence of $T_{\rm re}$ on $n_{\rm S}$ and p. Note that the lower bound on the reheating temperature is arrived at from the BBN constraints as $T_{\rm BBN} \sim 10$ MeV (see Refs. [13–15]; for a recent discussion, see Ref. [75]), whereas the upper limit comes from the condition of instantaneous reheating which corresponds to the inflationary energy scale of the order of the GUT scale of about 10^{16} GeV that arises in certain supersymmetric theories.

Let us emphasize a few more points concerning Fig. 6. It is clear that the new effective EOS parameter we have arrived at lowers the reheating temperature. This effect can be attributed to the dependence of $T_{\rm re}$ on the ratio $(1+w_{\rm eff})/(3w_{\rm eff}-1)$, which is always higher than the one computed with $w_{\rm eff} = w_{\rm co} = (p-2)/(p+2)$ for a given value of p. Thus, our proposal for the time-dependent EOS and its effect can, in principle, be tested in future experiments [76,77]. Moreover, note that, the variation of $T_{\rm re}$ with p also depends on the value of the scalar spectral index. It is evident from Fig. 6 that, for $p < 4$, an increase in the value of $n_{\rm S}$ results in a larger value of $T_{\rm re}$. This is due to the fact that for $p < 4$, $w_{\rm eff} < 1/3$ and, hence, an increase in the value of $n_{\rm S}$ leads to a smaller value of $N_{\rm re}$ which, in turn, leads to a larger value of $T_{\rm re}$. However, for $p > 4$, the conditions are reversed and we have a decreasing $T_{\rm re}$ for an increasing $n_{\rm S}$.

V. DISCUSSION

In this work, we have computed the effective EOS parameter during the reheating phase of the Universe by taking into account the time evolution of the instantaneous EOS parameter. We have shown that the gradient and interaction energy densities force the instantaneous EOS parameter to deviate from its value during the phase of coherent oscillations which succeeds inflation. Assuming that the inflationary potential behaves as $V(\phi) \propto \phi^p$ about its minimum, based on results from lattice simulations, we have argued that, during reheating, w increases monotonically and approaches $1/3$ for $p < 4$, whereas, for $p > 4$, it decreases monotonically to $1/3$ (cf. Fig. 4). In order to capture such a behavior, we have proposed two different functional forms of the time varying EOS parameter during reheating (cf. Fig. 5). We find that the resulting value of $w_{\rm eff}$ depends only on the inflationary model parameter p and is largely independent of the parametrizations we have considered for $w(N)$ (cf. Table I).

Let us stress here a few further points concerning the results we have obtained. Note that, in our approach, $w_{\rm eff}$ is *completely* determined by the inflationary parameter p. Therefore, for a specific p, the reheating temperature $T_{\rm re}$ is fixed for a given value of the scalar spectral index $n_{\rm S}$. This should be contrasted with earlier studies, wherein there is an arbitrariness in choosing the value of $w_{\rm eff}$. As we discussed earlier, often $w_{\rm eff}$ is either assumed to lie in the range $-1/3 \le w_{\rm eff} \le 1$ or simply taken to be same as that of $w_{\rm co}$. However, various (p)reheating studies have indicated towards time varying EOS, which has been captured efficiently with our parametrization. With such a time varying EOS parameter, we can uniquely define $w_{\rm eff}$ which, as we highlighted, is fixed by the behavior of the field around the minimum of the potential. It is worth stressing again that the $w_{\rm eff}$ we have arrived at is largely independent of parametrization. Thus, this study mitigates the arbitrariness in defining the effective EOS parameter during reheating for a given inflationary model.

Lastly, note that, though we have worked with the α-attractor model of inflation specified by the potential (25), our analysis applies to all the inflationary models that behave as ϕ^p around their minima. With ongoing and forthcoming CMB missions expected to constrain the inflationary parameters more accurately, we believe that our proposal for the time-dependent EOS during reheating can be well tested in the near future.

ACKNOWLEDGMENT

The authors thank Debaprasad Maity for fruitful discussions. P. S. wishes to thank the Indian Institute of Technology Madras, Chennai, India, for support through the Institute Postdoctoral Fellowship. S. A. is supported by the National Postdoctoral Fellowship of the Science and Engineering Research Board (SERB), Department of Science and Technology (DST), Government of India (GOI). L. S. wishes to acknowledge support from SERB, DST, GOI through the Core Research Grant No. CRG/2018/002200.

APPENDIX: BEHAVIOR OF THE EOS PARAMETER DURING PREHEATING

In order to highlight the behavior of the EOS parameter during the epoch of coherent oscillations that immediately follows inflation, in this Appendix, we shall briefly discuss the well known case of perturbative reheating in the popular quadratic inflationary potential (in this context, see also Refs. [25,27,28]). Incidentally, the perturbative mechanism we shall discuss here is the original idea of reheating, as we had mentioned in the introduction [16]. In this case, to transfer the energy from the inflaton to radiation, an additional damping term is introduced by hand in the equation governing the inflaton in the following fashion:

$$\ddot{\phi} + 3H\dot{\phi} + \Gamma_\phi\dot{\phi} + V_\phi = 0, \tag{A1}$$

Physically, the damping term is expected to arise due to quantum particle creation as the inflaton decays into other lighter species that are coupled to it. For instance, if ϕ is allowed to decay into fermionic channels via an Yukawa interaction of the form $\mathcal{L}_{\rm int} \supset g\phi\bar{\psi}\psi$, then, using the methods of perturbative quantum field theory, one can show that [78]

$$\Gamma_\phi \equiv \Gamma_{\phi\to\bar{\psi}\psi} = \frac{g^2 m_\phi}{8\pi}, \tag{A2}$$

where m_ϕ is the tree-level mass of the inflaton. Since we require a radiation dominated universe after reheating, for simplicity, it is often assumed that the inflaton directly transfers it's energy to radiation. In order to conserve the total energy of the systems involved, as a consequence of the additional decay term in the equation of motion (A1) of the inflaton, the equation describing the conservation of energy density ρ_γ of radiation is modified to be

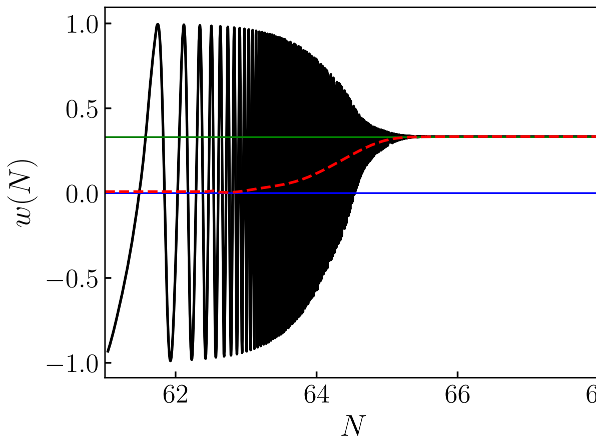

FIG. 7. The behavior of the instantaneous EOS parameter (in black) as well as the corresponding quantity arrived at after averaging over the oscillations (in orange) have been plotted for the case of the popular quadratic inflationary potential. We have set the value of the decay width to be $\Gamma_\phi = 2\times 10^{-9}\,M_{\rm Pl}$ in arriving at these plots. Note that the averaged EOS parameter starts at $w = 0$ (indicated by the blue horizontal line) and eventually approaches $1/3$ (indicated by the green horizontal line) suggesting the eventual transfer of energy from the inflation to radiation.

$$\dot{\rho}_\gamma + 4H\rho_\gamma - \Gamma_\phi\dot{\phi}^2 = 0, \tag{A3}$$

while the Hubble parameter H is governed by the following Friedmann equation:

$$H^2 = \frac{1}{3M_{\rm Pl}^2}\left(\frac{\dot{\phi}^2}{2} + V(\phi) + \rho_\gamma\right). \tag{A4}$$

The system of Eqs (A1) and (A3) can be readily solved with the initial conditions on the inflaton imposed at end of inflation and the initial radiation density assumed to be zero. The exact EOS parameter for the system is defined as

$$w = \frac{\frac{1}{2}\dot{\phi}^2 - V(\phi) + \frac{1}{3}\rho_\gamma}{\frac{1}{2}\dot{\phi}^2 + V(\phi) + \rho_\gamma}. \tag{A5}$$

We have plotted the EOS parameter during preheating for the case of the quadratic potential in Fig. 7. It is clear that the additional coupling introduced by hand transfers the energy from the inflation to radiation fairly effectively, in fact within a matter of a few e-folds.

[1] A. H. Guth, Phys. Rev. **23**, 347 (1981); Adv. Ser. Astrophys. Cosmol. **3**, 139 (1987).
[2] A. A. Starobinsky, Phys. Lett. **91B**, 99 (1980); Adv. Ser. Astrophys. Cosmol. **3**, 130 (1987).
[3] A. D. Lindee, Phys. Lett. **108B**, 389 (1982); Adv. Ser. Astrophys. Cosmol. **3**, 149 (1987).
[4] C. L. Bennett *et al.* (WMAP Collaboration), Astrophys. J. Suppl. Ser. **148**, 1 (2003).
[5] H. V. Peiris *et al.* (WMAP Collaboration), Astrophys. J. Suppl. Ser. **148**, 213 (2003).
[6] P. A. R. Ade *et al.* (Planck Collaboration), Astron. Astrophys. **571**, A16 (2014).
[7] P. A. R. Ade *et al.* (BICEP2 and Planck Collaborations), Phys. Rev. Lett. **114**, 101301 (2015).
[8] S. W. Hawking, Phys. Lett. **115B**, 295 (1982).
[9] A. H. Guth and S. Y. Pi, Phys. Rev. Lett. **49**, 1110 (1982).
[10] A. A. Starobinsky, Phys. Lett. **117B**, 175 (1982).
[11] J. M. Bardeen, P. J. Steinhardt, and M. S. Turner, Phys. Rev. **28**, 679 (1983).
[12] D. H. Lyth and A. Riotto, Phys. Rep. **314**, 1 (1999).
[13] M. Kawasaki, K. Kohri, and N. Sugiyama, Phys. Rev. Lett. **82**, 4168 (1999).
[14] G. Steigman, Annu. Rev. Nucl. Part. Sci. **57**, 463 (2007).
[15] B. D. Fields, P. Molaro, and S. Sarkar, Chin. Phys. C **38**, 339 (2014).
[16] A. Albrecht, P. J. Steinhardt, M. S. Turner, and F. Wilczek, Phys. Rev. Lett. **48**, 1437 (1982).
[17] L. F. Abbott, E. Farhi, and M. B. Wise, Phys. Lett. **117B**, 29 (1982).
[18] A. D. Dolgov and A. D. Linde, Phys. Lett. **116B**, 329 (1982).
[19] J. H. Traschen and R. H. Brandenberger, Phys. Rev. D **42**, 2491 (1990).
[20] L. Kofman, A. D. Linde, and A. A. Starobinsky, Phys. Rev. Lett. **73**, 3195 (1994).
[21] Y. Shtanov, J. H. Traschen, and R. H. Brandenberger, Phys. Rev. D **51**, 5438 (1995).
[22] D. T. Son, Phys. Rev. **54**, 3745 (1996).
[23] L. Kofman, A. D. Linde, and A. A. Starobinsky, Phys. Rev. **56**, 3258 (1997).
[24] D. Boyanovsky, M. D'Attanasio, H. J. de Vega, R. Holman, D. S. Lee, and A. Singh, arXiv:hep-ph/9505220.
[25] J. Martin and C. Ringeval, Phys. Rev. D **82**, 023511 (2010).
[26] M. S. Turner, Phys. Rev. **28**, 1243 (1983).
[27] V. Mukhanov, *Physical Foundations of Cosmology* (Cambridge University Press, Oxford, 2005).
[28] D. I. Podolsky, G. N. Felder, L. Kofman, and M. Peloso, Phys. Rev. D **73**, 023501 (2006).
[29] R. Micha and I. I. Tkachev, Phys. Rev. Lett. **90**, 121301 (2003).
[30] R. Micha and I. I. Tkachev, Phys. Rev. D **70**, 043538 (2004).
[31] R. Allahverdi, R. Brandenberger, F.-Y. Cyr-Racine, and A. Mazumdar, Annu. Rev. Nucl. Part. Sci. **60**, 27 (2010).
[32] M. A. Amin, M. P. Hertzberg, D. I. Kaiser, and J. Karouby, Int. J. Mod. Phys. D **24**, 1530003 (2015).
[33] D. G. Figueroa and F. Torrenti, J. Cosmol. Astropart. Phys. 02 (2017) 001.
[34] D. Maity and P. Saha, J. Cosmol. Astropart. Phys. 07 (2019) 018.
[35] K. D. Lozanov and M. A. Amin, Phys. Rev. Lett. **119**, 061301 (2017).
[36] K. D. Lozanov and M. A. Amin, Phys. Rev. **97**, 023533 (2018).
[37] J. B. Munoz and M. Kamionkowski, Phys. Rev. D **91**, 043521 (2015).
[38] E. Komatsu *et al.* (WMAP Collaboration), Astrophys. J. Suppl. Ser. **192**, 18 (2011).
[39] P. A. R. Ade *et al.* (Planck Collaboration), Astron. Astrophys. **594**, A20 (2016).
[40] Y. Akrami *et al.* (Planck Collaboration), Astrophys. Space Sci. **364**, 69 (2019).
[41] J. Martin, C. Ringeval, and V. Vennin, Phys. Rev. Lett. **114**, 081303 (2015).
[42] L. Dai, M. Kamionkowski, and J. Wang, Phys. Rev. Lett. **113**, 041302 (2014).
[43] J. L. Cook, E. Dimastrogiovanni, D. A. Easson, and L. M. Krauss, J. Cosmol. Astropart. Phys. 04 (2015) 047.
[44] M. Drewes, J. U. Kang, and U. R. Mun, J. High Energy Phys. 11 (2017) 072.
[45] J.-O. Gong, S. Pi, and G. Leung, J. Cosmol. Astropart. Phys. 05 (2015) 027.
[46] D. Maity and P. Saha, Phys. Rev. **98**, 103525 (2018).
[47] D. Maity and P. Saha, Phys. Dark Universe **25**, 100317 (2019).
[48] R. Allahverdi, K. Dutta, and A. Maharana, J. Cosmol. Astropart. Phys. 10 (2018) 038.
[49] D. Maity and P. Saha, Classical Quantum Gravity **36**, 045010 (2019).
[50] A. Di Marco, G. De Gasperis, G. Pradisi, and P. Cabella, Phys. Rev. D **100**, 123532 (2019).
[51] R. Kallosh and A. Linde, J. Cosmol. Astropart. Phys. 07 (2013) 002.
[52] G. N. Felder and I. Tkachev, Comput. Phys. Commun. **178**, 929 (2008).
[53] G. N. Felder, Comput. Phys. Commun. **179**, 604 (2008).
[54] S. Antusch, D. G. Figueroa, K. Marschall, and F. Torrenti, arXiv:2005.07563.
[55] N. Seto and J. Yokoyama, J. Phys. Soc. Jpn. **72**, 3082 (2003).
[56] S. Weinberg, *Gravitation and Cosmology* (John Wiley and Sons, New York, 1972).
[57] J. J. M. Carrasco, R. Kallosh, and A. Linde, J. High Energy Phys. 10 (2015) 147.
[58] J. J. M. Carrasco, R. Kallosh, and A. Linde, Phys. Rev. **92**, 063519 (2015).
[59] V. F. Mukhanov, H. A. Feldman, and R. H. Brandenberger, Phys. Rep. **215**, 203 (1992).
[60] J. Martin, Braz. J. Phys. **34**, 1307 (2004).
[61] J. Martin, Lect. Notes Phys. **669**, 199 (2005).
[62] B. A. Bassett, S. Tsujikawa, and D. Wands, Rev. Mod. Phys. **78**, 537 (2006).
[63] L. Sriramkumar, Curr. Sci. **97**, 868 (2009), http://www.jstor.org/stable/24112121.
[64] L. Sriramkumar, in *Vignettes in Gravitation and Cosmology*, edited by L. Sriramkumar and T. R. Seshadri (World Scientific, Singapore, 2012), pp. 207–249.
[65] D. Baumann, in *Physics of the Large and the Small, TASI 09, Proceedings of the Theoretical Advanced Study Institute*

in Elementary Particle Physics, Boulder, Colorado, USA, 2009 (World Scientific, Singapore, 2011), pp. 523–686.
[66] A. Linde, in *100th Les Houches Summer School: Post-Planck Cosmology: Les Houches, France, 2013*, Les Houches Lect. Notes Vol. 100 (2015), pp. 231–316.
[67] J. Martin, Astrophys. Space Sci. Proc. **45**, 41 (2016).
[68] J. Garcia-Bellido, D. G. Figueroa, and J. Rubio, Phys. Rev. **79**, 063531 (2009).
[69] J. Repond and J. Rubio, J. Cosmol. Astropart. Phys. 07 (2016) 043.
[70] K. Freese, E. I. Sfakianakis, P. Stengel, and L. Visinelli, J. Cosmol. Astropart. Phys. 05 (2018) 067.
[71] R. Easther, R. Flauger, and J. B. Gilmore, J. Cosmol. Astropart. Phys. 04 (2011) 027.
[72] N. Musoke, S. Hotchkiss, and R. Easther, Phys. Rev. Lett. **124**, 061301 (2020).
[73] R. Allahverdi and A. Mazumdar, J. Cosmol. Astropart. Phys. 10 (2006) 008.
[74] G. N. Felder and L. Kofman, Phys. Rev. D **63**, 103503 (2001).
[75] T. Hasegawa, N. Hiroshima, K. Kohri, R. S. L. Hansen, T. Tram, and S. Hannestad, J. Cosmol. Astropart. Phys. 12 (2019) 012.
[76] F. Finelli *et al.* (CORE Collaboration), J. Cosmol. Astropart. Phys. 04 (2018) 016.
[77] S. Kuroyanagi, K. Nakayama, and J. Yokoyama, Prog. Theor. Exp. Phys. **2015**, 13E02 (2015).
[78] M. D. Schwartz, *Quantum Field Theory and the Standard Model* (Cambridge University Press, Cambridge, England, 2014).